

14. M. Grin's P. I. Kripyakevich, and Ya. P. Yarmolyuk, *Visnik L'viv. Univ., Ser. Khim.* No. 17, 12 (1975).
 15. L. Smirnova, *Kristallografiya* **1**, 165 (1956) [*Sov. Phys. Crystallogr.* **1**, 128 (1956)].
 16. I. Gladyshevskii, I. I. Zalutskii, and G. T. Tivanchuk, *Visnik L'viv. Univ., Ser. Khim.* No. 14, 9 (1972).
 17. I. Kripyakevich and Ya. P. Yarmolyuk, *Dopovidi Akad. Nauk. UkrSSR, Ser. A*, 460 (1974).
 18. Amfelt and A. Westgren, *Jernkontorets Ann.* **119**, 185 (1935).
 19. C. Brink Shoemaker and D. P. Shoemaker, *Acta Crystallogr.* **23**, 231

(1967).
 18. P. I. Kripyakevich, *Kristallografiya* **18**, 730 (1973) [*Sov. Phys. Crystallogr.* **18**, 460 (1974)].
 19. I. I. Zalutskii, E. E. Cherkashin, O. I. Zalutskaya, and P. I. Kripyakevich, *All-Union Conf. on the Crystal Chemistry of Intermetallic Compounds, Summaries of Reports [in Russian]*, *Izd. L'vov Gos. Univ., L'vov* (1971), p. 25.
 20. P. I. Kripyakevich, *Zh. Strukt. Khim.* **16**, 631 (1975).

Translated by G. D. Archard

Tundrite, $\text{Na}_2\text{Ce}_2\text{TiO}_2[\text{SiO}_4](\text{CO}_3)_2$ — refinement of the crystal structure and chemical formula

N. G. Shumyatskaya, A. A. Voronkov, V. V. Ilyukhin, and N. V. Belov

Institute of Crystallography, Academy of Sciences of the USSR

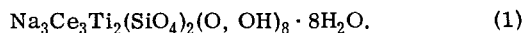
(Submitted January 13, 1976)

Kristallografiya **21**, 705–715 (July–August 1976)

As a result of a refinement of the crystal structure of tundrite (based on a new x-ray experiment) a changed chemical formula is established for this mineral; tundrite has become a representative of a comparatively rare family of minerals, the silico-carbonates.

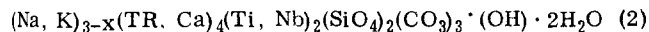
PACS numbers: 61.50.Qy, 61.10.Fr

Preliminary information as to the structure of the complex silicate tundrite was presented in an earlier paper.¹ Following an incomplete chemical analysis and subsequent examination by x-ray diffraction (the diffraction pattern being recorded photographically), the mineral was given the formula



A new discovery of tundrite² has now presented analysts with an adequate amount of good-quality material, facilitating a more precise determination of the chemical composition of this mineral, one of the characteristic components being carbonic acid (this was subsequently also found in samples obtained from different sites), so that now tundrite occupies an important position in the interesting family of silico-carbonates, hitherto having only a limited number of representatives.

Processing of the new chemical analyses leads² to the general formula



or approximately $\text{NaO}_4\text{Ce}_4\text{Ti}_2(\text{SiO}_4)_2(\text{SO}_3)_3\text{O}_4 \cdot (\text{OH}) \cdot 2\text{H}_2\text{O}$. Comparison with ref. 1 shows that the anion half of the formula has altered considerably; a considerable proportion of the oxygen atoms have passed into the carbonate groups $(\text{CO}_3)^{2-}$, with a corresponding reduction in the manner of neutral H_2O molecules.

It should be noted that the relatively poor accuracy of the determination of the intensities in ref. 1 (using the photographic method) and its inevitable consequence (diffuse maxima on the electron-density maps) prevented reliable separation of the light elements C and O in the presence of the extremely heavy Ce atoms ($Z_{\text{Ce}}/Z_{\text{C}} \approx 10$, $Z_{\text{Ce}}/Z_{\text{O}} \approx 7$), either by reference to the R factors or by

reference to the heights of the $\rho(xyz)$ peaks. Since the chemical data were incomplete we had to regard some of the anions appearing in the $\rho(xyz)$ maps as neutral water molecules because of their considerable valence under-saturation, revealed when calculating the Pauling valence balance.¹ Nevertheless, the total number of O anions in the formula established by x-ray and purely chemical methods practically coincided.

The changed formula of tundrite made it essential to repeat the structural investigation using independent experimental material. We used single crystals of Khibinsk tundrite² corresponding to the most accurate chemical analysis available. The 3700 independent $F_{\text{hk}0}^2 - F_{\text{hk}5}^2$ were recorded in a Syntex P1 automatic diffractometer without any absorption correction, the omission being justified by the lamellar form of the sample (the great brittleness of the mineral prevented any machining). The refined parameters of the triclinic cell were $a = 7.560 \pm 0.002$; $b = 13.957 \pm 0.003$; $c = 5.040 \pm 0.001$ Å; $\alpha = 101^\circ 07' \pm 10'$; $\beta = 70^\circ 52' \pm 10'$; $\gamma = 100^\circ 01' \pm 10'$.

The three-dimensional P(uvw) function (Fig. 1) was solved by the multiple-peak method.³ The initial vector was the one indicated as I in the figure (intensity about 1000 relative units) with coordinates $u = 0.13$ $v = 0.44$ $w = 0.10$. Using the principles indicated in ref. 4, we established the multiplicity of this vector as 2. The construction of $M_3(\text{I}, \text{I}) = M\{M_2(\text{I}) \cdot [M_2(\text{I})]\}$ led to a vector system of the first order^{5,6} and this was taken as the new vector sum P'. Expansion of the latter with respect to vector II (Fig. 1) left one point in $M_3(\text{II}, \text{II}) = M\{[M_2(\text{II})] \cdot [M_2(\text{II})]\}$, where $[M_2(\text{II})] = M\{P', P'\}$. Thus (in conformity with ref. 7) the parallelogram based on vectors I and II becomes unique in the main system of coordinates and may be chosen as the separating polygon.⁸ Since the original displacement vectors I and II are the strongest in the P(uvw) map, it is

TABLE I. Coordinates, Temperature Parameters (B), Multiplicities μ , and Relative Values of ρ for the Basic Atoms ($B_{\text{tot}} = 0.88 \text{ \AA}^2$, $R_{\text{hkl}} = 0.07$, F.g. p1)

Atoms	x/a	y/b	z/c	$B, \text{\AA}^2$	μ	ρ
Ce(1)	0.6565	0.7787	0.5923	0.83	1.99	1009
Ce(2)	0.2181	0.7776	0.3103	1.04	1.97	935
Ti	0.6100	0.9997	0.1947	0.10	2.15	368
Si	0.9610	0.8578	0.9115	0.37	2.00	203
Na(1)	0	0	0.5000	1.82	0.99	82
Na(2)	0.1405	0.4747	0.1748	2.08	1.97	78
Na(3)	0.5000	0.5000	0.5000	3.26	0.91	65
C(1)	0.7914	0.3534	0.2433	1.22	1.94	40
C(2)	0.5993	0.6535	0.0623	0.71	1.97	55
O(1)	0.9335	0.7563	0.7068	0.66	2.00	63
O(2)	0.7925	0.9172	0.9089	0.81	2.00	70
O(3)	0.1613	0.9167	0.7245	0.70	2.00	79
O(4)	0.9563	0.8430	0.2243	0.88	2.00	61
O(5)	0.4053	0.9185	0.0677	0.81	2.00	71
O(6)	0.5504	0.9189	0.4993	0.74	2.00	72
O(7)	0.8735	0.3813	0.9915	0.01	2.00	46
O(8)	0.8096	0.4043	0.4623	2.41	2.00	48
O(9)	0.3343	0.3761	0.7702	1.46	2.00	57
O(10)	0.4046	0.3923	0.1771	1.37	2.00	65
O(11)	0.3076	0.7558	0.7489	1.24	2.00	73
O(12)	0.5458	0.7415	0.1339	0.91	2.00	70

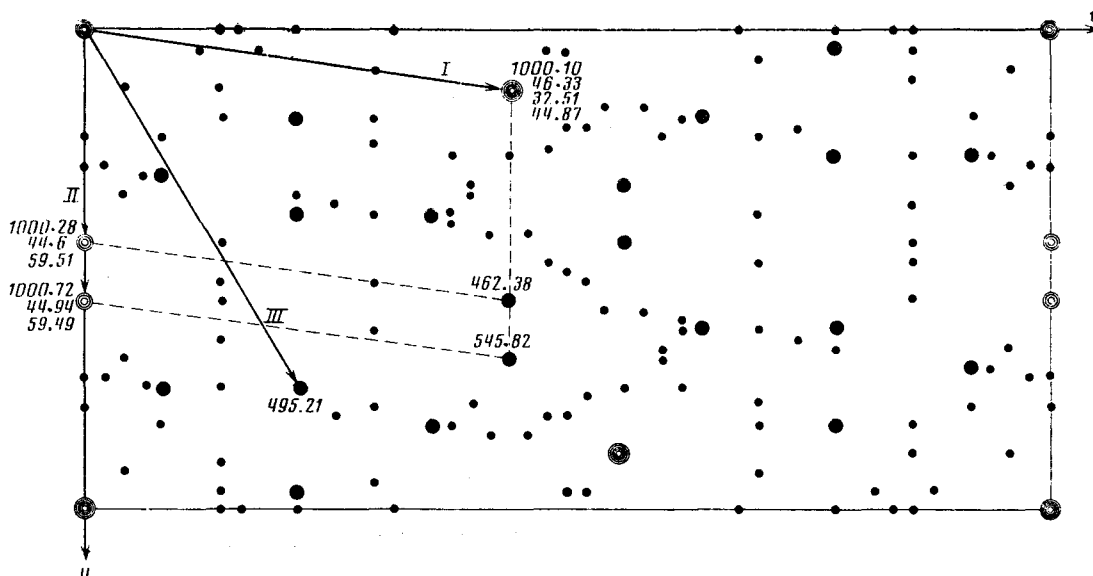


Fig. 1. Tundrite. Three-dimensional Patterson function $P(uvw)$; of the two numbers appearing adjacent to some of the maxima, the first gives the weight in relative units and the second gives the height w in hundredths of the c axis. The arrows indicate the displacement vectors I, II, and III. The dashed line indicates the separating polygon (parallelogram (two different choices of parallelogram are shown, leading to two identical copies of the basic system but displaced relative to one another).

natural to assume that the vertices of the parallelogram in question are the ends of the Ce-Ce vectors.

The resultant $M_4 = M\{M_2(I)[M_2(II)]\}$ gave two copies of the basic system - direct and inverse - and in order to eliminate of these yet another vector was added to the peak-separating parallelogram, until a maximum having a centrosymmetrical twin analog was obtained in M_4 (vector III in Fig. 1). Ultimately in $M_5 = M\{M_4(I, II), M_2(III)\}$ we established 22 points, of which eight (four corresponding to Ce atoms, plus four taken as Ti and Si atoms) were used to calculate the phases when constructing the first electron-density synthesis $\rho(xyz)$ (R factor $\approx 24.8\%$ $B = 0$). Twelve new maxima coinciding with those separated in M_5 were introduced when constructing the second synthesis ($R = 23.1\%$), in which all the light atoms of the structure were located. Allowance for the latter in the final $\rho(xyz)$ distribution reduced the R factor to 21.5%. The reliability of the placing of the atoms was monitored by reference to

the $P(uvw)$ distribution, and also by reference to the difference series of $\Delta\rho(xyz)$ (the contributions of the heavy Ce, Ti, and Si atoms being subtracted).

The model obtained at the present stage of solution confirmed the validity of the structural base established in ref. 1; it includes all the high-valence cations (apart from C) and also the whole oxygen matrix of the structure and a high proportion of the Na atoms. A new feature of special importance was the sharp revelation of the C atoms in the form of typical triangles and also yet another large cation of low scattering power (absent from the earlier model), which was taken as Na^+ .

The "x-ray" content of the cell corresponded to the formula $\text{Na}_4\text{Ce}_4\text{Ti}_2\text{Si}_2\text{C}_4\text{O}_{24}$, which again lay outside the framework of the latest chemical analysis² by reason of the extra Na and C atoms (one of each), even without considering the protons H^+ . A further characteristic of the

TABLE 2. Interatomic Distances and Valence Angles in the Tundrite Structure

Atoms	Distances, Å	Angles, O—Me—O	Atoms	Distances, Å	Angles, O—Me—O
Ce(1) —1	2.43		Si —1	1.62	
Ce(1) —2	2.56		Si —2	1.65	
Ce(1) —4	2.54		Si —3*	1.65	
Ce(1) —6	2.42		Si —4*	1.61	
Ce(1) —9	2.57		1 —2	2.58	103°40'
Ce(1) —10	2.73		1 —3*	2.56	102°49'
Ce(1) —11	2.48		1 —4*	2.72	114°33'
Ce(1) —12	2.64		2 —3*	2.64	106°00'
Ce(1) —12*	2.69		2 —4*	2.74	113°48'
Ce(2) —1	2.42		3*—4*	2.75	114°42'
Ce(2) —3	2.58		Na(1) —2	2.46(×2)	
Ce(2) —4	2.52		Na(1) —3	2.45(×2)	
Ce(2) —5	2.45		Na(1) —4	2.41(×2)	
Ce(2) —7	2.58		Na(2) —7	2.53	
Ce(2) —8	2.91		Na(2) —8	2.55	
Ce(2) —11	2.70		Na(2) —9	2.46	
Ce(2) —11*	2.67		Na(2) —10	2.49	
Ce(2) —12	2.46		Na(2) —7*	2.34	
Ti —2*	2.01		Na(2) —8*	2.34	
Ti —6	1.95		Na(3) —8	2.85(×2)	
Ti —5	1.95		Na(3) —9	2.30(×2)	
Ti —3*	2.01		Na(3) —10	2.22(×2)	
Ti —5*	1.93		C(1) —7	1.31	
Ti —6*	1.96		C(1) —8	1.24	
2*—6	2.94	95°55'	C(1) —11	1.32	
2*—5	2.77	88°51'	7—8	2.24	123°08'
2*—3*	2.74	86°09'	7—11	2.23	115°47'
2*—5*	2.94	96°42'	8—11	2.23	121°00'
3*—5*	2.91	94°57'	C(2) —9	1.27	
6 —5*	2.73	89°12'	C(2) —10	1.27	
6 —3*	2.94	96°07'	C(2) —12	1.32	
3*—6*	2.78	88°59'	10—9	2.25	124°17'
6 —6*	2.52	80°29'	10—12	2.23	118°23'
5*—6*	2.71	88°18'	9—12	2.21	117°04'
5 —5*	2.52	80°45'			
5 —6*	2.91	96°49'			

The numbers in the "atoms" column denote O atoms belonging to the twelve crystallographic complexes (Table 1). The asterisk denotes atoms derived from basic symmetry operations. The angular quantities O—Me—O are expressed as angles based on the corresponding edges of the polyhedra.

new model is the centrosymmetrical distribution of all the atoms in the cell, without any exception, despite the fact that all the preliminary calculations were carried out in the acentric P1 group. The existence of the x-ray symmetry center contradicted the appearance of a piezo-effect in tundrite crystals.¹ At the later stages of the structural analysis these contradictions thus also had to be solved. The least-squares refinement of the working model was therefore executed within the framework of both space groups (P1 and P $\bar{1}$) in relation to the positional and thermal parameters and also the real multiplicities of the positions occupied by Ce³⁺, Na⁺, and C. The resultant R factors for the acentric and centrosymmetrical groups were almost the same, 0.064 and 0.070, respectively. The average deviations of the refined coordinates of the acentric model from their ideal values in the P $\bar{1}$ group were no greater than 0.02 Å for the heavy and 0.06 Å for the light atoms, while the paired averaging of the positional parameters of atoms linked by a "pseudocenter" practically reproduced the coordinates of the centrosymmetrical version (Table 1).¹ The interatomic distances (Table 2) in the second case were far more logical than in the acentric model, especially in the C triangles. Thus within the framework of the P1 group the C—O bond lengths vary from the too-short value of 1.11 Å to the anomalously long 1.39 Å; the lengths of the O—O edges vary over the range 2.17–2.28 Å, and the valence angles O—C—O over the range 113–133°. In the P $\bar{1}$ group the corresponding values were 1.24–1.32, 2.21–2.25 Å, and 116–120°. In the centrosymmetrical aspect of the structure, the unnaturally short-ended Na—O distances were eliminated, and the

lengths of the bonds in the tetrahedra were equalized.

Thus within the accuracy limits of our x-ray experiments the structure of tundrite is centrosymmetrical and may be described within the framework of the P $\bar{1}$ Fedorov group. The existence of the piezo-effect (if existing indications of this are valid) is clearly associated with finer nuances of the structure, not susceptible to x-ray analysis.²⁾

The refined true multiplicities of the cations in the

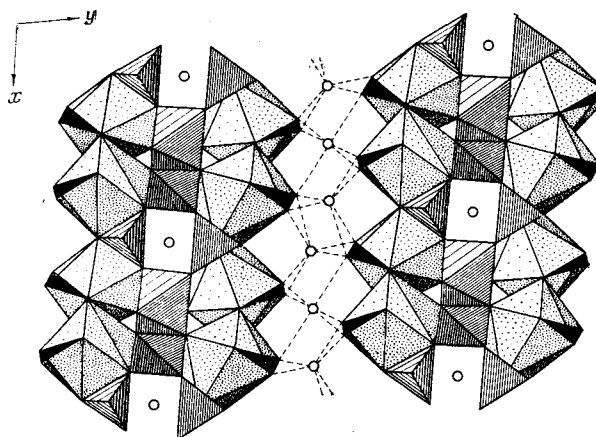


Fig. 2. Tundrite. Projection of the structure in polyhedra on the (001) plane. The ends of the Ti—Si—O network (shaded) are shown, together with walls of Ce polyhedra (dotted). The circles represent Na cations, the black triangles CO₃ groups. The dashed lines indicate Na—O bonds.

two versions of the structure practically coincide with the ideal values for the corresponding Fedorov groups; we are thus compelled to accept the presence of four alkali cations and four carbon atoms in the cell. In the finally accepted centrosymmetrical model (Table 1) the occupation factors μ in the one-fold positions amount to 0.91 and 0.99, and in the two-fold positions 1.97; for the two independent C atoms we have 1.94 and 1.97 (2 in the ideal situation). The conclusion as to the even number of these atoms is also supported by the ordinary and difference syntheses of $\rho(xyz)$ plotted on the basis of the previously refined coordinates. Peaks of approximately the same intensity correspond to independent atoms of the same chemical nature (in the one-fold complexes of the P1 group). Although the structural analysis favored the $\bar{P}1$ Fedorov group and the new cell content to a high degree of reliability, the presence of heavy Ce atoms ($Z = 58$) in the cell nevertheless gave grounds for internal dissatisfaction. The influence of the Ce atoms on the character of the intensity distribution in the F^2 series and then on the electron-density distribution was decisive: The centrosymmetrical disposition of these in the cell might lead to a false centrosymmetrical arrangement of the model as a whole, leading to the "appearance" of light atoms (C in particular) on the $\rho(xyz)$ maps, although these were in fact absent. The reasonably accurate measurement of the experimental intensities, however, ($R_{hkl} = 0.064$) enabled us to construct differential Patterson syntheses with coefficients $[F_e - F_3Ce + 2Ti + 2Si]^2$ and $F_e^2 - F_4Ce + 2Ti + 2Si$; these yielded four sharp independent Ce-Na vectors and also four independent Ce-C vectors, i.e., once again the centrosymmetrical nature of tundrite and the material content of its cell, $Na_4Ce_4Ti_2Si_2C_4O_{24}$ were confirmed.

Instead of the three Na atoms and three C atoms indicated by chemical analysis, the tundrite cell contains four of each, and the molecules of constitutional water are in fact absent. We cannot fail to note that if, in the chemical analysis of the mineral,² the sum of all the losses incurred while roasting (earlier ascribed to H_2O) is added to the percentage CO_2 content, the total number of C atoms in the cell becomes equal to 4. We may add that the tundrite structure does not contain any large spaces capable of accommodating extra water molecules (apart from the 24 oxygen atoms already located).

Let us now consider isomorphic substitution in the group of cations. The chief impurity elements in tundrite are Ca and Nb. The first isomorphically replaces the large

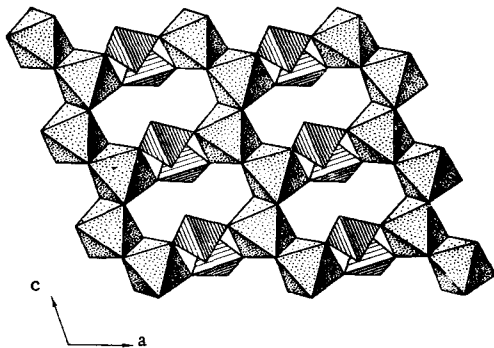


Fig. 3. Tundrite. Titanium-silicon-oxygen network in projection on the (010) plane.

Ce cation while the second enters into the Ti octahedra on the principle of heterovalent isomorphism: $Ce^{3+} + Ti^{4+} \rightleftharpoons Ca^{2+} + Nb^{5+}$. An indirect indication of this may be given by the μ values of the corresponding basic atoms (Table 1), to which the standard f curves corresponding to uncharged Ce and Ti atoms were attributed during the structure calculation. According to the resultant values of μ , most of the Ca enters into the nine-pointed polyhedra of Ce(2), which have a lower ρ maximum than Ce(1) and a greater temperature factor B_j . We note that, in refining the acentric version of the structure, preferential Ce \rightarrow Ca substitution was only established for one of the four independent Ce atoms, which suggests a selective type of isomorphism in relation to the latter (this also constitutes a potential cause of the reduction in the symmetry of the tundrite structure). Allowing for these main impurities, formula (2) may be expressed in the form



The two independent Ce atoms are situated in large nine-pointed polyhedra of irregular shape with distances Ce-O 2.42-2.91 Å. The titanium atoms lie in distorted octahedra with Ti-O 1.93-2.01 Å; among the O-O edges, two are shortened to 2.52 Å, and along these edges neighboring Ti octahedra are connected into an infinite column of the brookite type. The individual Si tetrahedra are practically regular, with Si-O = 1.61-1.65 Å. The cations Na(1) and Na(3), lie in large oxygen octahedra with distances Na(1)-O 2.41-2.46 Å and Na(3)-O 2.22-2.85 Å. The coordination polyhedra around the Na(2) are distorted trigonal pyramids with Na(2)-O = 2.34-2.55 Å. The ordinary C triangles are considerably distorted: C-C = 1.24-1.32 Å for edge lengths O-O 2.21-2.24 Å. The O-C-O valence angles fluctuate from $115^\circ 47'$ to $124^\circ 17'$.

The crystal structure of tundrite represents a completely new type, never before encountered among natural minerals. The layer-like character stands out very sharply in projection on the (001) plane (Fig. 2). Ranks of Ti column parallel to the [001] are pinned by Si orthotetrahedra to form a skeletal wall, a layer-like radical of the $\{Ti_2O_4 \cdot [SiO_4]_2\}_{\infty}^{8-} = \{TiSiO_6\}_{\infty}^{4-}$ type, in which all the vertices are separated from their radical partners in the case of the Ti octahedra but only half in that of the Si tetrahedra,

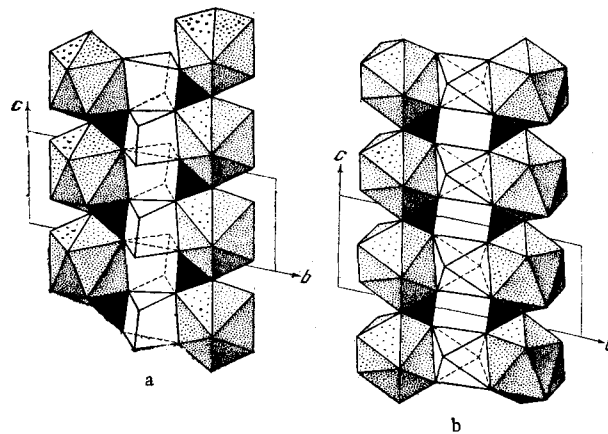


Fig. 4. Tundrite. Three-layer panel of large Ce and Na polyhedra. The cross sections of the panel are parallel to the $(\bar{2}10)$; a) at the level $x = 0.25$; b) at the level $x = 0.5$. The black triangles are CO_3 carbonate groups.

as in Fig. 3. The Ti columns neighboring each other in the mixed radical are translationally identical along the [100] direction; they are mutually connected in a direction perpendicular to the [101] chain axis by a (solely crystallographically) mirror plane,³⁾ so that large gaps remain (loop against loop) between them (Fig. 3), covered top and bottom by pairs of Si tetrahedra and occupied by an Na(1) cation in the octahedral coordination; the Na octahedron rests with its central section on the edges of tetrahedra lying crosswise, while its "trans"-vertices are closed by the free ("suspended" in the mixed radical) vertices of two other Si tetrahedra. This type of building-in of the alkali cations into a titanium-silicon-oxygen network appears characteristically in the layer-like structures of lomonosovite,⁹ vuonnemite,¹⁰ and innelite.¹¹

Between the "anion" networks lying at a translation of $b \sim 14 \text{ \AA}$ from one another (Fig. 2) are three-layer "cation" panels of large Ce and Na polyhedra, "larded" with CO_3 carbonate groups. Inside this complex fragment of structure the layer-like properties once again appear quite clearly. The outer continuous walls of the panel are formed by twelve-pointed Ce polyhedra connected by common edges in the direction of the a axis (7.5 \AA) and by vertices along the c axis (Figs. 2 and 4). The central layer is made up of Na polyhedra of two kinds: trigonal prisms and octahedra. These appear in Fig. 4a, b, which illustrates two successive vertical sections parallel to the $(\bar{2}10)$ plane; each of these passes through Ce polyhedra connected by an inversion center and made up of Ce, Na, and C atoms of one crystallographic variety. The Na(2) prisms, coupled along the edges of their triangular bases (Fig. 4a), form an infinite zigzag column along the c axis. Within the cross section each prism has a common vertical edge with a Ce(2) polyhedron and another with a Ce(1) triangle. The latter also borders two neighboring (along the z direction) twelve-pointed Ce polyhedra and is "compressed" between the shortened edges of three large polyhedra. The vertical edge of the Na prism projecting from the plane of the sketch is shortened, forming the edge of a C(2) triangle from the neighboring section. Each Na prism borders four CO_3 groups: one along the edge and two at the vertices.

The mutual disposition of the Ce(1) polyhedra and the associated carbonate groups (Fig. 4b) practically reproduce the scheme already described, but instead of the continuous columns of Na(2) prisms we have a rank of discrete set-on-edge Na(3) octahedra alternating with flattened empty polyhedra of similar configuration. The vertical edges of the latter form the edges of the C(2) triangles and simultaneously of the Na(2) prisms. The Na(3) octahedra themselves are in contact at the vertices with six carbonate groups. The tips of the octahedra projecting from the plane of the sketch are linked to the C(1) triangles from the neighboring section. The Na(3) octahedron shares its "vertical" edges with the neighboring Ce(1) polyhedra and some of the inclined edges with the Na(2) prisms.

The whole three-story layer in the structure of tundrite constitutes a fairly monolithic construction comprising the coordination polyhedra of large cations cemented with CO_3 groups. The bond forces within this structure are distributed in a nonuniform way. The stronger Ce-

O (and especially C-O) bonds are concentrated in the outer sheets of the panel; the inner Na layer is only characterized by the weak Na-O bond forces, and these are responsible for the perfect cleavage of the tundrite crystals along the (010).

It is quite proper to treat the tundrite structure as "antimica"; the characteristic three-layered packets within it are represented by a core of Ti and Si polyhedra [with additional $\text{Na}(1)^+$ ions] and the outer leaves by cerium walls cemented with CO_3 triangles. The Na(2) and Na(3) ions become "fillers" of the interpacket space, through which the splitting of the crystals into plates takes place (Fig. 2).

The crystal habit, involving compression along the (010) plane, agrees with the layer-like character of the structure. The elongation of the crystals along the c axis is determined by the columns of Ti octahedra and Na(2) prisms. The structural characteristics of the mineral also explain its optical properties. In tundrite (by analogy with pure carbonates) the character of the birefringence is mainly determined by the orientation of the CO_3 groups. The planes of these are practically parallel to the z axis. Since the polarization of the electron shells of the oxygen atoms in the carbonate ion reaches a maximum in the plane of the ion, the greatest refractive index n_g should coincide with the [001]. On the other hand, the planes of the C triangles make a maximum angle with the crystallographic a axis; along this axis (or its projection $a \sin \beta$) we may expect the smallest index n_p . The contrast between n_g and n_p should increase still further on account of the Ti chains along the [001] direction.

This agrees completely with the optics of tundrite, and explains, in particular, the extremely large (and rare for silicates) value of $n_g - n_p = 0.12$. As regards n_m , unfortunately this quantity has not been established experimentally. The corresponding axis of the indicatrix is directed along the normal to the (010) (the plane of the optic axes) and makes a small angle of 10° with the b axis. Figure 4b shows that there is no preferential orientation of the carbonate groups in the direction in question; how-

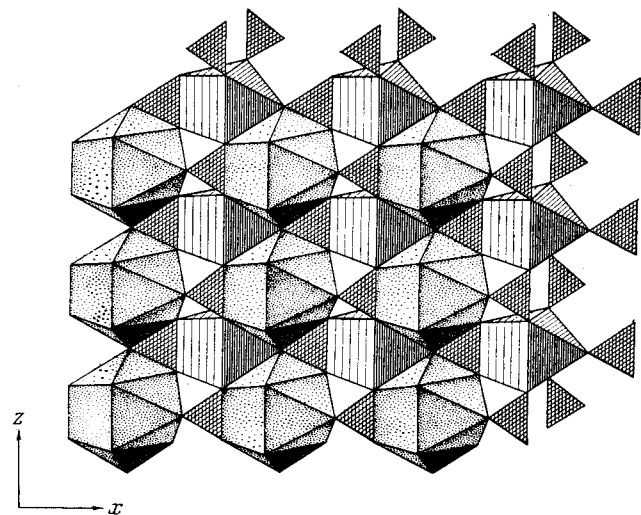


Fig. 5. Carbobarnaite. Fragment of the structure in projection on the (010) plane. Wall of Ce and Na (Ca) polyhedra with built-in C triangles.

TABLE 3. Local Balance of Valences in Tundrite

Anion	Na(1)	Na(2)	Na(3)	Ce(1)	Ce(2)	Ti	Si	C(1)	C(2)	Σ
O(1)				1/3	1/3		1			12/3
O(2)	1/6			1/3		2/3	1			21/6
O(3)	1/6				1/3	2/3	1			21/6
O(4)	1/6			1/3	1/3		1			15/6
O(5)						2/3+2/3				12/3
O(6)				1/3	1/3	2/3+2/3				12/3
O(7)		1/6+1/6			1/3			1/3		2
O(8)		1/6+1/6	1/6		1/3			1/3		21/6
O(9)		1/6	1/6	1/3					1/3	2
O(10)		1/6	1/6	1/3					1/3	2
O(11)				1/3	1/3+1/3			1/3		21/3
O(12)				1/3+1/3	1/3				1/3	21/3

ever, the planes of the independent C triangles make quite a large angle with one another (over 60°) and this weakens (extinguishes) the influence of the CO₃ groups when light passes along the b axis, and correspondingly the index n_m should be closer to n_p than to n_g , which agrees with the established positive optical sign of the tundrite crystals $n_g - n_m > n_m - n_p$.

For all the individuality of the atomic structure of tundrite, certain specific structural features are very much the same as in other crystal structures of silicates. Among the representatives of the small class of silico-carbonates there are no close relatives of tundrite. In the rare earth kainosite¹² Ca₂TR₂Si₄O₁₂(CO₃)H₂O carbonate groups are built in between the shortened edges of neighboring Ti polyhedra in the same way as in tundrite. However, on the whole kainosite is organized on a different motif with discrete four-fold [Si₄O₁₂] rings.

It is interesting to compare tundrite with the rare earth carbonate carbocernaite¹³ (Na, Ca) (TR, Sr)(CO₃)₂, since the two minerals have something in common as regards their motifs (Fig. 5). The Ce walls in the two structures are practically identical (they are slightly corrugated in carbocernaite).⁴ This is reflected in the closeness of the corresponding lattice constants in the plane of the TR wall of both minerals $a = 7.56$; $c = 5.04 \text{ \AA}$ in tundrite and $a = 7.30$, $c = 5.23 \text{ \AA}$ in carbocernaite. Between the TR layers are the less compact walls of Na (tundrite) and (Na, Ca) carbocernaite) polyhedra. The base of the latter is composed of trigonal prisms, which in the carbonate are built up to form seven-pointed polyhedra. However, the chains of the polyhedra in question are drawn out in a direction differing from that in tundrite, namely, along the b axis. As in tundrite (see above), half of all the C triangles of carbocernaite are characterized by the same surroundings; they are "compressed" between the shortened edges of three large polyhedra — two Ce and one (Na, Ca). The spatial orientation of the carbonate groups is also analogous: parallel to the shortest 5 Å translation and almost perpendicular to the 7 Å. The optical characteristics are similar, although with the important difference that the mean index n_m of carbocernaite is closer to n_g than to n_p .

However, while noting the similarity between the central panels of tundrite and carbocernaite, we must not fail to mention the differences associated with the different stoichiometry of the motifs under comparison. The "cation" layer of tundrite contains a superfluous Na atom (in discrete octahedra), whereas for each TR atom of carbo-

cernaite there are not one but two CO₃ groups. The necessary valence compensation in tundrite is achieved by virtue of the side sheets of the panel — the "anion" titanium-silicon-oxygen networks $\{Ti_2O_4[SiO_4]_2\}_{\infty\infty}^{8-}$.

CONCLUSIONS

Despite certain indications as to the qualitative detection of a piezo-effect in tundrite crystals, the structure of this mineral is described by the centrosymmetrical Fedorov group $P\bar{1}$, within the limits of the accuracy set by x-ray analysis. The hitherto uncertain chemical composition of tundrite may now be regarded as basically solved. Tundrite is a complex alkali silico-carbonate of titanium and the rare earth elements (principally cerium), without any hydroxyl groups or neutral water molecules; this follows from the complete balance of valences presented in Table 3. The high refractive indices $n_g = 1.880$, $n_p = 1.761$ also bear witness against the presence of structurally bound water in this mineral.²

¹The thermal parameters fell within the norm set for the error in both cases.

²One reason for the fall in symmetry may be isomorphic substitution of the atoms, to be considered later.

³This arrangement of neighboring brookite chains appears here for the first time. In brookite itself (within the limits of a single layer) these columns repeat one another in a direction normal to the axis of the Ti chains. A picture analogous to that of brookite is encountered in columbite and the pyroxenes; in the motifs of these the corresponding columns are constructed from Nb and Mg (Fe, Mn) octahedra.

⁴The coordination number of the TR in carbocernaite is increased to 10, but in tundrite also, in addition to the nine closest O neighbors, the Ce atom has yet another additional ligand, at a distance of 3.17 Å.

¹N. G. Shumyatskaya, A. A. Voronkov, V. V. Ilyukhin, and N. V. Belov, Dokl. Akad. Nauk SSSR 185, 1289 (1969) [Sov. Phys. Dokl. 14, 304 (1969)].

²Z. V. Shlyukova, E. V. Vlasova, M. E. Kazakova, G. O. Piloyan, N. G. Shumyatskaya, and B. E. Boruski, Dokl. Akad. Nauk SSSR 211, 426 (1973).

³V. P. Golovachev, Yu. N. Drozdov, V. V. Ilyukhin, É. A. Kuz'min, A. N. Chernov, and N. V. Belov, Kristallografiya 16, 725 (1971) [Sov. Phys. Crystallogr. 16, 631 (1972)].

⁴É. A. Kuz'min, V. V. Ilyukhin, and N. V. Belov, Zh. Strukt. Khim. 11, 943 (1970).

⁵É. A. Kuz'min, V. V. Ilyukhin, and N. V. Belov, Zh. Strukt. Khim. 12, 643 (1971).

⁶É. A. Kuz'min, A. A. Petrunina, V. V. Ilyukhin, and N. V. Belov, Dokl. Akad. Nauk SSSR 206, 343 (1972).

⁷É. A. Kuz'min, Dissertation [in Russian], Rostov State Univ., Rostov-on-Don (1974).

⁸J. M. Burgers, Structure of Crystals and Vector Space [Russian translation], IL, Moscow (1961).

⁹R. K. Rastvetaeva, V. I. Simonov, and N. V. Belov, Dokl. Akad. Nauk SSSR 177, 832 (1967) [Sov. Phys. Dokl. 12, 1090 (1968)].

¹Yu. N. Drozdov, N. G. Batalieva, A. A. Voronkov, and É. A. Kuz'min, Dokl. Akad. Nauk SSSR 216, 78 (1974) [Sov. Phys. Dokl., 19, 258 (1973)].
²A. N. Chernov, B. A. Maksimov, V. V. Ilyukhin, and N. V. Belov, Kristallografiya 16, 87 (1971) [Sov. Phys. Crystallogr., 16, 65 (1971)].
³G. F. Volodina, I. M. Rumanova, and N. V. Belov, Dokl. Akad. Nauk

SSSR 149, 173 (1963).
¹³A. A. Voronkov and Yu. A. Pyatenko, Zh. Strukt. Khim., 8, 935 (1967).

Translated by G. D. Archard

Crystal-structural illustrations of Shubnikov antisymmetry groups

Yu. G. Zagal'skaya, G. P. Litvinskaya, and N. V. Belov

M. V. Lomonosov Moscow State University

(Submitted February 11, 1976)

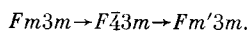
Kristallografiya 21, 716-721 (July-August 1976)

Models of crystal structures in which geometrically equivalent and identically situated polyhedra are nevertheless physically and chemically different (empty and occupied, or occupied by atoms of different kinds) are interpreted in terms of Shubnikov antisymmetry groups (black-and-white or plus-and-minus symmetry). Certain "hard sphere" models are also considered on the same principle.

PACS numbers: 61.50.Em, 61.50.Gp

In one of our earlier papers¹ the Shubnikov groups were illustrated exclusively by structures in which the "coloring" was determined by a sequence of geometrically identical occupied and empty polyhedra. The only example in which such polyhedra were "tinted" in two colors by virtue of different "fillings" was chalcopyrite, considered as a superstructure with respect to sphalerite. In this paper the number of such examples will be considerably extended.

In the sphalerite-chalcopyrite pair both the Fedorov (F43m-I42d) and the Shubnikov (Fm'3m-I'42d) groups are different. However, if we pass from sphalerite to the NaZnAs type of structure, replacing S by As and filling the tetrahedra which were empty in sphalerite with Na atoms, neither the Fedorov (F43m) nor the Shubnikov (Fm'3m) group will alter. The NaZnAs type of structure may also be regarded as a superstructure to the anti-fluorite structure (for example, to Li₂O); the "color" interpretation then, as it were, restores the lost symmetry of the original structural type:



Both the Fedorov group (R3m) and the Shubnikov group (R'3m), are also preserved in the pair CdCl₂ (= CdCl₂)—NaFeO₂, since the latter may be obtained by filling the vacant layers of the octahedral spaces of the CdCl₂ structure.

As indicated earlier,¹ the polyhedral representation of the NaCl structure does not enable us to visualize any color-symmetry elements; however, these may be expected to appear in superstructures of NaCl. Thus the NaFeO₂ structure just considered may be linked not only with CdCl₂ but also with NaCl, if in the latter we "color" layers of octahedra perpendicular to one of the three-fold axes, so that instead of Fm_{3m} (NaCl) we obtain R3m and R'3m (NaFeO₂).

Another superstructure of NaCl is LiInO₂, in which each layer of octahedra of the NaCl structure perpendicular to one of the four-fold packing axes is occupied by Li and In atoms on the chessboard principle. The structure

becomes tetragonal with a Fedorov group I4₁/amd (*a*LiInO₂ = *a*NaCl, *a*LiInO₂ = 2*c*NaCl). In the Shubnikov group of LiInO₂ the lattice is centered in a colored manner (I'4₁/amd), which results in the "duplicity" (simultaneity) of the planes *d* (*d* ≡ *d*' and *d** ≡ *d*')¹ and hence of the single-thread, four-fold axes (4₁ ≡ 4₃' and 4₃ ≡ 4₁').

The groups I(4₁/a)md, and especially R3m are among those in which color symmetry appears by virtue of positions characterized by a single symmetry, lying at distances equal to the translational vector of the color lattice from one another. Also interesting in this respect is the diamond group O_h⁷ (Fd3m), in which a $\bar{T}/2$ shear characterizes both the 8*a*-8*b* (symmetry 43m) and the 16*c*-16*d* (symmetry 3m) positions. This is effectively realized in the spinel structure, in which beams of aluminum octahedra (position 16*d*) drawn out along the face diagonals of the cube alternate with similar beams of empty octahedra (16*c*), shifted by $\bar{T}/2$; of the two tetrahedral positions the only occupied one is the (8*a*), in which the tetrahedra are created by the faces of the octahedra in the empty beams,

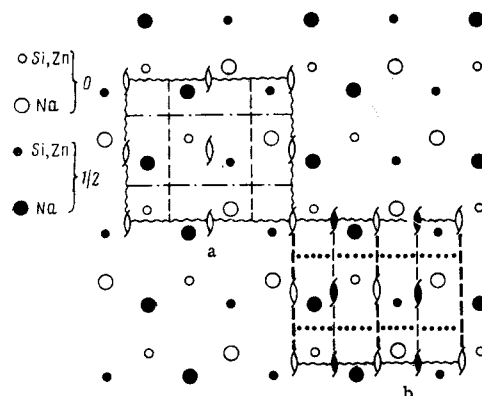


Fig. 1. Fedorov (a) and Shubnikov (b) groups in the idealized Na₂ZnSiO₄ structure. The circles correspond to the centers of the sodium and zinc-silicon tetrahedra. The classical symmetry elements are indicated by the thin lines and light symbols, the antisymmetry elements by the thick lines and dark symbols.